Ab Initio-Derived Dynamics for F_2 Reactions with Partially Fluorinated Si(100) Surfaces: Translational Activation as a Possible Etching Tool

Lawrence E. Carter and Emily A. Carter*

Department of Chemistry and Biochemistry, University of California, Los Angeles, California 90095-1569

Received: September 29, 1995[⊗]

We have investigated via ab initio-derived molecular dynamics simulations the influence of up to 4.0 eV of translational excitation on the reactivity of F_2 molecules with the Si(100) surface. We propose a stepwise reaction mechanism which yields two pathways involving Si−F bond formation: F atom abstraction, where one Si−F bond is formed at the expense of the F−F bond while the remaining F atom is ejected from the surface, and dissociative chemisorption, where both F atoms in the incident F_2 molecule form Si−F bonds in a consecutive fashion, once again at the expense of the F−F bond. For the clean surface, we find abstraction to be highly probable at low incident energies, with increasing translational kinetic energy in impinging F_2 molecules leading to increased dissociative chemisorption at the expense of atom abstraction and thus higher reactivity. We do not observe nonreactive scattering for the clean surface, where the incident F_2 molecule reflects from the surface without forming an Si−F bond, but this changes with the introduction of preadsorbed fluorine on the surface. We observe decreasing reactivity with increasing surface fluorine coverage, eventually leading to minimal reactivity for surfaces with 1 ML of fluorine coverage. The reactivity can be increased both by increasing F_2 translational kinetic energy and the introduction of disorder to the silicon surface. We also characterize the products which are ejected from the surface during our simulations. We find that F atoms generated during abstraction have hyperthermal energies which are not characteristic of the surface temperature and exhibit minimal memory of the F_2 incident energy. F_2 molecules which undergo nonreactive scattering do demonstrate memory of their initial conditions, but their exit energy is reduced relative to their incident energy due to the inelastic nature of the scattering. Both types of ejected species have exit angular distributions which are indicative of their nonequilibrated natures. On the basis of our simulations, we predict that translationally activated F_2 molecular beams may be effective for applications involving neutral beam etching of silicon surfaces.

I. Introduction

The importance of plasma etching in the fabrication of microelectronic devices continues to provide a driving force for research into reactions on semiconductor surfaces. Plasmas containing fluorine or other halogens are commonly used in industry to selectively etch technologically important silicon surfaces, such as the Si(100) surface. In spite of this widespread industrial use, the complex nature of the plasma etching environment has contributed to difficulties in characterizing the reaction mechanisms involved in etching. As a result, the basic reactions in the etching process remain unknown.

Since the plasma etching environment has eluded direct characterization, experimentalists have turned to molecular beam studies as simplified, model systems for studying etching reaction mechanisms.[1] Molecular beam techniques provide a method for delivering reagents to a substrate with a specified incident energy and angle. This fine control over the reactants facilitates finding barriers to reactivity, scattered product angular distributions, and other features which provide insight into the reaction mechanisms occurring on the surface. Ultimately the goal is to use this information about basic reaction mechanisms to build up an understanding of the full etching environment.

Several choices are available for the type of fluorine-containing agent to be used in a beam experiment studying reactions with the Si(100) surface. Atomic fluorine is one logical choice, as it is present in the plasma etching environment.[2] However, beams of pure atomic fluorine are difficult to generate. Instead, beams containing atomic fluorine also tend to contain a large amount of a precursor, such as F_2, from which the atomic fluorine was produced. XeF_2 has been proposed as an alternative to atomic fluorine in molecular beam experiments.[3−8] Beams of pure XeF_2 are easier to generate than beams of atomic fluorine, and fluorine atoms delivered to a Si(100) surface in the form of XeF_2 are thought to exhibit reactivity similar to that of atomic fluorine. However, the role of the Xe atoms or the metastable XeF intermediates in the reaction, if any, is still unclear at this time.

The reaction of F_2 molecules with a Si(100)-2×1 surface provides a more easily characterized starting point for building an understanding of plasma etching of Si(100) with fluorine. Current molecular beam techniques can generate essentially monoenergetic beams containing only F_2 and an inert carrier gas, such as He. Thus, all of the reactions and scattered products produced from a molecular beam of F_2 impinging on Si(100) surface can be attributed solely to F_2 interacting with the silicon surface. The one possible drawback is that F_2 is much less reactive toward the Si(100) surface than atomic fluorine. While F atoms will spontaneously etch an Si(100) surface at room temperature, thermal molecular fluorine eventually passivates a room temperature silicon surface.[9]

Only a few experimental studies of molecular beams of F_2 molecules impinging on the Si(100) surface have been reported in the literature. The most comprehensive study is due to Engstrom et al.[10] They used X-ray photoelectron spectroscopy to analyze Si(100) surfaces dosed via an effusive F_2 molecular beam source, in order to study the reactivity of both F atoms and F_2 molecules with Si(100) surfaces as a function of incident

* To whom correspondence should be addressed.

[⊗] Abstract published in *Advance ACS Abstracts,* December 15, 1995.

0022-3654/96/20100-0873$12.00/0

kinetic energy in the impinging beam, surface temperature, and surface coverage. They found an initial adsorption probability, S_0, for F_2 on the clean Si(100) surface of 0.46 ± 0.02 for F_2 beams with incident center-of-mass (COM) translational energies ranging from 0.07 to 0.83 eV and a surface temperature of T_{surf} = 298 K. The incident energies may be somewhat misleading, however, as their beam impinged on the surface at 75° from the surface normal, yielding incident energies normal to the surface ($E_n = E_i \cos^2 \Theta_i$) of at most 0.06 eV. (It is thought that the normal component of the energy is often the relevant quantity in characterizing surface reactions, so-called "normal energy scaling".) They also reported that this value for S_0 was independent of the surface temperature. In addition to these direct reactivity measurements, Engstrom et al. also provided some analysis of the mechanisms and kinetics involved in F_2 adsorption on Si(100). For $T_{surf} > 200$ K, they reported a second-order coverage dependence in the rate of adsorption of fluorine. Below 200 K, they found a lower coverage dependence and attributed this to an extrinsic precursor state, an adsorption precursor state where $F_{2(g)}$ resides above an already occupied adsorption site, which is only populated at sufficiently low temperatures.

More recent work by Ceyer and co-workers, which appeared in a review article,[1,11] provides evidence for the importance of normal energy scaling. Using thermal desorption as a probe, Ceyer and co-workers measured the amount of SiF_2 and SiF_4 formed on Si(100)-2×1 as a function of COM translational kinetic energy in the incident F_2 molecules. They reported that the yield of SiF_4 increased when the surface was dosed with F_2 molecules having incident energies normal to the surface greater than 0.16 eV. From helium atom scattering structural data, they deduced that this barrier may be due to insertion of fluorine atoms both into Si−Si dimer bonds on the surface and into Si−Si bonds between atoms in adjacent layers. (A description of the silicon surface can be found in section II.) In a separate publication, Li et al. reported on changes in the adsorption of F_2 as a function of fluorine coverage (Θ_F).[12] They observed initial adsorption probabilities on the clean Si(100) surface of 0.91 ± 0.02 for an incident energy of 0.03 eV using time-of-flight mass spectrometry. As the coverage on the surface increased, they found a decrease in adsorption probability, eventually leading to an adsorption probability of 0 for a surface with Θ_F = 1 ML (ML = monolayer). Ceyer and co-workers have also found increases in the initial adsorption probability with increasing translational kinetic energy in the incident F_2 molecules.[13]

Behringer, Flaum, and Kummel have performed a similar set of studies to those of Ceyer.[14] They also used thermal desorption to investigate the influence of incident F_2 translational kinetic energy on SiF_4 formation and found greatly enhanced yields of SiF_4 when the incident energy increased from 0.060 to 0.275 eV, in agreement with Ceyer and co-workers' measurements.[11] They attributed this increase to a barrier as well, but Behringer et al. suggested this barrier is only to insertion into bonds between Si atoms in consecutive layers, rather than also into the Si−Si dimer bonds. Initial adsorption probabilities on the clean surface, S_0, were also mentioned in another work by Behringer et al.[15] They report $S_0 = 0.58$ for F_2 molecules with an incident energy of 0.060 eV, while an incident energy of 0.275 eV leads to an S_0 of 0.78.

In spite of the relatively small range (<1 eV) of F_2 incident energies studied, the results of Ceyer and co-workers[13] and Behringer et al.[14] show evidence for increased reactivity with increasing incident COM translational energy for the F_2 molecules. Similar trends have also been observed for the interaction of Cl_2 with the Si(100) surface, where a much wider range of incident energies have been studied.[16] Incident energies up to 6 eV have been reported, and several studies have shown substantially higher etch rates for Cl_2 beams with incident energies above 2 eV. The higher incident energy studies are particularly interesting, since as we will speculate later, hyperthermal molecular beams may eventually be useful for anisotropic, damage-free etching. Using translational activation to overcome barriers, instead of using a more reactive substance, means that the impinging etchant particle will be highly reactive only when it first strikes the surface. If the particle does not react during its first collision, its translational energy will be reduced. This might prevent it from scattering away and then reacting with and damaging either other parts of the surface or the sidewalls of the etch feature. This type of damage would lead to undesirable reductions in anisotropy, as the feature would grow laterally on the surface as well as into the surface.

An additional benefit of using molecular beam studies for investigating the reaction of F_2 molecules with the Si(100)-2×1 surface is that these studies are also accessible to theoretical methods, specifically molecular dynamics (MD) simulations. The traditional molecular beam experiment consists of impinging a beam of molecules (F_2) onto a surface (Si) for a period of time. Although these molecules strike the surface consecutively, the reaction events are basically independent of one another. (The time between two F_2 molecules striking a given localized area on the surface is long relative to the time scale of the reaction.) We will use a slightly different method in our simulations. Rather than simulating many F_2 molecules impinging on a Si(100) surface consecutively in time, we will model many trajectories of exactly identical Si(100) surfaces, each interacting with a single F_2 molecule. In our simulations of the interaction of F_2 molecules with the clean surface, each F_2 molecule is assigned a predetermined incident kinetic energy and a random location and orientation above the surface. The initial condition of the surface is truly identical for each trajectory, so that the only difference between two trajectories is the initial condition of the F_2 molecule. Thus, our simulations not only generate independent events, but we also have the advantage of knowing the exact state of the surface at the start of each trajectory. In this manner we will build up statistics for the interaction of F_2 molecules having a variety of incident energies with a Si(100) surface in the ultimate low-pressure limit. Additionally, we will repeat this procedure with several Si(100) surfaces to study the differences in reactivity between the clean Si(100) surface and surfaces with various numbers of fluorine atoms already adsorbed on the surface. While our theoretical study is not exactly identical to a molecular beam experiment, it is similar enough to allow direct comparison to these experiments and thus provide further insight into current and future experimental results.

Stillinger and Weber reported the first simulation of this type for F_2 interacting with Si(100), in conjunction with their development of an empirical interatomic potential for simulating the interactions between Si and F.[17−19] While a large amount of solid state and gas phase data were available for fitting the pure Si and pure F interactions,[17,18] respectively, Stillinger and Weber were forced to use gas phase SiF_x and Si_2F_x data to fit the Si−F cross terms in the potential.[19] Using ab initio calculations on embedded Si clusters interacting with up to four F atoms to model the surface reactions, Wu and Carter showed that the resulting Si−F interaction potential underestimated the strength of the Si−F interaction while overestimating the nonbonded repulsions between adsorbed fluorosilyl groups, causing the potential to be overly repulsive in nature.[20,21] As a

result, Weakliem, Wu, and Carter parametrized a new Si−F potential using the Stillinger−Weber functional form.[22,23] We used this new potential in a previous work to show that, for F_2 interacting with the clean Si(100)-2×1 surface, the Weakliem, Wu, and Carter (WWC) potential provided qualitatively different results than the Stillinger−Weber (SW) potential and that the WWC potential more closely matched current experimental findings.[24] Schoolcraft et al. carried out similar simulations for a clean Si(100)-2×1 surface at 1000 K using both the WWC and SW potentials and reported similar results.[25] We will discuss pertinent aspects of our previous simulations below in conjunction with the results of our current work. Additionally, we have also used the WWC potential to show that the reactivity of F_2 toward the Si(100) surface is largely insensitive to the presence of steps or dimer vacancy defects on the surface.[26,27]

A few other types of theoretical studies of the interaction of atomic or molecular fluorine with the Si(100) surface are reported in the literature. Schoolcraft and Garrison used the original SW potential to consecutively bombard an Si(100) surface with 3.0 eV F atoms.[28] They predicted these high-energy F atoms would spontaneously etch the Si(100)-2×1 surface, demonstrating at least a limited ability of these simulations to reproduce the experimental observation of spontaneous etching by thermal F atoms. Barone and Graves also used the SW potential with an additional potential to account for the interaction of argon ions to study the properties of disordered SiF_x layers when bombarded with high-energy Ar^+ ions.[29] Feil et al. provided another application of molecular dynamics to etching in their study of the interaction of Cl_2 with the Si(100) surface.[30] Other studies of F atoms interacting with the Si(100) surface include semiempirical SLAB-MINDO calculations by Radny and Smith[31] and Craig and Smith.[32,33] The most recent work by Radny and Smith[31] studied $\Theta_F = 0.5$ and 1 ML on the Si(100) surface. Their calculations predicted that the most favorable location for an F atom on the $\Theta_F = 0.5$ ML surface was at a bridge site between two dimers within a single row, and for $\Theta_F = 1$ ML they predicted that one F atom would lie in the bridge site with the second F atom in a terminal (single Si) site, in contrast to the ab initio GVB-CI calculations of Wu and Carter[20,21] and current experimental evidence,[34−36] which indicate adsorption occurs at terminal sites only. Lastly, a related simulation involves Cl_2 on Si(111). Stich et al. performed five ab initio molecular dynamics trajectories, each with a different orientation of Cl_2 approaching the Si(111) surface, where the forces were determined at each time step directly from density functional theory using the local density approximation.[37,38] They predicted that Cl_2 dissociatively chemisorbs on the surface and noted that although changing the orientation of the Cl−Cl bond axis relative to the surface changed the dynamics, the resulting dissociated state was independent of initial orientation. This is in contrast to our findings for F_2 on clean Si(100), where the orientation of the F_2 was found to have a strong effect on the relative positions of the adsorbed F atoms.[24]

In the remainder of this paper, we will present the results of molecular dynamics simulations of F_2 molecules interacting with a variety of Si(100) surfaces. Section II will provide the specific details of our simulation method. Section III contains the primary results and analysis of the MD simulations, including our predictions for the reaction mechanism. Section IV illustrates how these simulations of well-characterized molecular beam scattering can lead to new understanding of and design principles for etching of silicon. Section V provides a concluding summary of our findings.

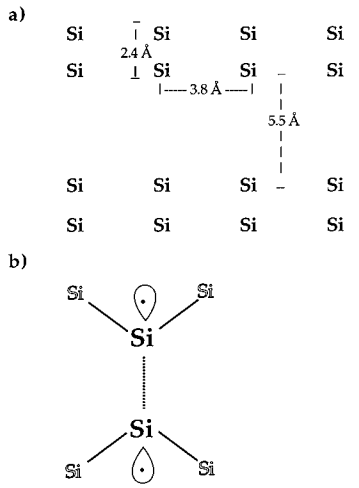

Figure 1. (a) Schematic of the dimer row reconstruction present on Si(100) surfaces. The distances between two Si atoms within a dimer, Si atoms in adjacent dimers within a row, and Si atoms in dimers in adjacent rows. (b) Schematic top view of a single Si dimer. Each **Si** atom in a dimer has two bonds to Si atoms in the layer below, a third bond to the other **Si** atom in the dimer, and a "dangling bond" containing one electron.

II. Simulation Details

We used an ab initio-derived two- and three-body potential to describe the interactions between atoms. The pure silicon[17] and pure fluorine[18] interaction potentials are from the work of Stillinger and Weber (SW), who fit these potentials to empirical data and showed their validity for modeling bulk silicon and gaseous fluorine molecules. The terms in the potential involving both Si and F were of the SW functional form but fit to ab initio calculations on embedded clusters of silicon and fluorine by Weakliem, Wu, and Carter.[20−23] The clusters were specifically designed to model fluorine atoms interacting with a Si(100) surface as well as the repulsions between neighboring fluorines on the surface. In a previous study of fluorine reacting with the clean Si(100) surface, we demonstrated that this Stillinger−Weber style potential produced excellent qualitative agreement with available experimental data for F_2 interacting with clean Si(100).[24]

Before continuing with the next step in defining our simulations, which involves building the Si(100) surface, a brief description of the structure of the Si(100)-2×1 surface is in order. Figure 1a shows a schematic of a small portion of the top layer of a "reconstructed" Si(100) surface and the approximate distances between the closest types of neighboring atoms within the top layer. Although bulk silicon prefers a diamond lattice structure, when the (100) face is exposed, the surface "reconstructs" to form rows of dimers on the surface in order to minimize the number of broken bonds when the surface is created. After reconstruction, each silicon atom on the surface has two bonds to atoms in the layer below, a third bond to the other atom in the same dimer, and a "dangling bond", an orbital containing only one electron (Figure 1b). These dangling bonds are the primary reactive sites on the surface, and unless otherwise specified, all Si−F bonds formed during our simulations are formed at these sites. Due to the reconstruction, which causes the Si(100) surface to consist of rows of Si dimers instead of rows of atoms, the size of the unit cell for this surface is doubled in the direction of the dimerization. Thus, this surface is referred to as having "2 × 1" symmetry. We will return to this diagram shortly when we propose a mechanism for the reaction of F_2 with the Si(100) surface.

TABLE 1: F_2 Incident Energies (eV) Examined in This Work

translational	translational + vibrational	translational	translational + vibrational
0.078		1.500	
0.234	0.078 + 0.164	2.000	
0.364	0.078 + 0.286	2.500	
0.494	0.078 + 0.416	3.000	
0.642	0.078 + 0.564	3.500	
0.906	0.078 + 0.828	4.000	

The basic surface used in these simulations was a silicon slab nine layers thick containing 64 atoms per layer. This slab was placed in a tetragonal unit cell of dimensions 30.72 × 30.72 × 10.86 Å, with the (100) face of the crystal exposed in the direction of the shortest cell dimension. Periodic boundary conditions were enforced in the other two directions (parallel to the surface) in order to model an infinite surface. Each surface used in the simulations was initially forced to have the p(2×1) reconstruction found on the perfect Si(100) surface for the top layer of atoms. The surface was then equilibrated using a Nose−Hoover canonical ensemble algorithm[39,40] to achieve a velocity distribution characteristic of $T = 298$ K for the upper eight layers of the slab. The bottom layer of atoms was held fixed in ideal bulk positions during this equilibration. These atoms remained motionless during all subsequent equilibrations and simulations as well in order to represent the bulk crystal. (If this layer was allowed to move, it would also reconstruct to a geometry characteristic of a surface rather than a bulk layer of atoms.)

At this point fluorine atoms were added to the surfaces where initial fluorine coverage was desired. Surfaces with $\Theta_F = 0.5$ ML were generated by randomly choosing one Si atom from each dimer pair and placing a fluorine atom 2.0 Å above it. The surface was then equilibrated again using the Nose−Hoover scheme to allow the fluorine atoms to move and form Si−F bonds and then to restore the lattice temperature to 298 K. A similar procedure was utilized to create $\Theta_F = 1$ ML ordered surfaces, with the exception that every dangling bond site (instead of half of them) on the surface was fluorinated. Note that for both the $\Theta_F = 0.5$ and 1 ML ordered surfaces, no Si−Si dimer bonds were broken during this procedure. Thus, the $\Theta_F = 1$ ML ordered surface consists of ordered rows of surface F−Si−Si−F groups, as opposed to the ordered rows of Si dimers with two dangling bonds found on the clean surface, while still retaining the underlying 2 × 1 symmetry of the clean reconstructed Si(100) surface. Alternate $\Theta_F = 1$ ML surfaces which did not retain the underlying 2 × 1 structure of the Si surface dimers were also created. To create these $\Theta_F = 1$ ML "disordered" surfaces, we consecutively bombarded the Si(100)-2×1 surface with 1.5 eV translationally excited F atoms. More details about building the disordered surfaces are presented where the MD results are discussed for these surfaces. Although multiple surfaces were generated for each Θ_F, only one surface of each type was used in the calculations presented here. The alternate surfaces at each Θ_F were used to ensure that the calculations were reproducible and did not involve artifacts due to an unusual surface configuration.

Each trajectory started by placing a single F_2 molecule at a randomly chosen location above one of the previously equilibrated surfaces beyond the interaction range of any atoms on the surface. As mentioned above, the initial configuration of the silicon surface was identical for all simulations involving a particular value of Θ_F. The fluorine molecule was given an initial COM translational energy, and in some cases vibrational excitation, chosen from the list of initial conditions in Table 1. The COM velocity of the F_2 was directed normal to the surface, as in the experiments of Ceyer[11−13] and Kummel.[14,15] For cases without vibrational excitation, the atoms in the F_2 molecule were initially separated by 1.435 Å, the minimum energy in the Stillinger−Weber F−F potential. Vibrational energy was added to the F−F bond by positioning the F atoms farther apart, such that the initial F−F potential energy was above the potential energy minimum by the amount of the desired vibrational excitation. Zero initial rotational energy was provided to the diatomic to mimic the rotationally cold nature of a supersonic molecular beam. Similarly, the orientation of the F−F bond axis relative to the surface was chosen from a spherically symmetric distribution, as would be found experimentally.

All of our simulations were carried out in the microcanonical (constant number of particles, N, constant volume, V, and constant energy, E) ensemble so that the trajectories represent true classical dynamics. The majority of the trajectories were propagated forward in time using a simple Verlet algorithm[41] with an integration time step of 3.06536×10^{-16} s. (For incident energies >2.5 eV, the time step was reduced to 2.500×10^{-16} s.) The simulations were propagated until the trajectory of the F_2 could be classified as belonging to some reaction pathway (see below for pathway descriptions) and until any species ejected from the surface were beyond the interaction range of the surface. Typically, this involved about 1 ps of simulation time, although some trajectories required up to 6 ps for full characterization.

A total of 200 trajectories were performed for each initial condition described in Table 1. Two different methods were used to calculate error bars during data analysis. For averaged quantities, such as the average exit energy of scattered F_2 molecules, the error bars represent one standard deviation for the data. For quantities which are probabilities, such as the percentage occurrence of dissociative chemisorption, the error bars are computed using the formula $\sigma = [p(1 - p)/n]^{1/2}$, where σ is the error, p is the probability of the event occurring, and n is the total number of trajectories for a given initial condition, i.e., 200.[42]

We have used four basic styles of graphs to display and analyze the data generated by our simulations. The first type of graph displays the adsorption probability of F_2 molecules on a given surface as a function of the incident COM translational kinetic energy of the impinging F_2 molecule. The second type of plot shows the partitioning between reaction channels as a function of incident translational and/or vibrational energy for a given surface. In these graphs, the percentage occurrence of each reaction channel is plotted for each incident energy in order to elucidate reactivity trends and relationships between the reaction pathways. A third kind of graph displays the energy of F atoms and F_2 molecules which escape the surface after the interaction of the impinging F_2 molecule. For atomic fluorine we track only the translational energy of the escaping F atoms, while plots of both the translational and vibrational energy of exiting F_2 molecules are presented. The final type of plot also assists in characterizing scattered species by depicting the angular distribution of exiting F atoms or F_2 molecules for a particular Θ_F and F_2 incident energy. When displaying the angular distribution relative to the surface normal, we summed over all angles in the plane of the surface (azimuthal angles), and we similarly have summed over all angles relative to the surface normal when displaying azimuthal angular distributions. In order to display the distributions, the data were grouped into 5° or 10° bins.

III. Results and Discussion

The overwhelming majority of trajectories produced by our simulations can be classified as belonging to one of three

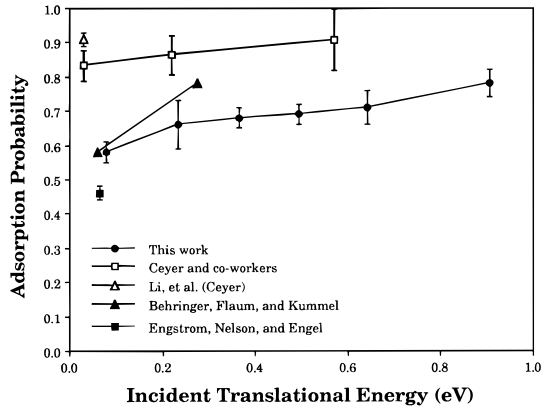

Figure 2. Comparison to experimental results for the initial adsorption probability, S_0. The adsorption probability is defined as the number of atoms which form Si−F bonds divided by the total number of F atoms which approach the surface (two per F_2 molecule). The horizontal axis shows the incident COM translational kinetic energy of the F_2 molecules.

reaction pathways: *F atom abstraction* occurs when one Si−F bond is formed at the expense of the F−F bond, with the remaining F atom ejected from the surface. In *dissociative chemisorption*, two Si−F bonds are formed on the surface, once again at the expense of the F−F bond. *Nonreactive scattering* does not result in the formation of any Si−F bonds. The F_2 molecule is ejected from the surface with its F−F bond intact. However, a few trajectories do fall outside of these categories. At higher incident F_2 COM translational energies, *collision-induced dissociation* occurs to a small degree. In this pathway, no Si−F bonds are formed, but the F−F bond is broken and the F atoms scatter independently from the surface. Our simulations also yield small amounts of *complex formation*. After the first Si−F bond is formed, occasionally the F−F bond will not break on the time scale of our simulation, yielding a metastable Si−F−F complex on the surface. The F atoms produced during collision-induced dissociation can also become trapped in this type of complex with a previously formed Si−F group. Ultimately, these physisorbed F_2 and F atom complexes will fall apart, simply at time scales longer than ∼10 ps.

As a calibration point, we first calculated the probability for the adsorption of F_2 on the clean Si(100)-2×1 surface as a function of incident translational energy in order to compare with experimental findings. Figure 2 shows the initial adsorption probability, S_0, as a function of incident F_2 COM translational kinetic energy as reported by Engstrom et al.,[10] Li et al.,[12] Ceyer and co-workers,[13] and Behringer et al.,[15] along with our predicted values. We define the adsorption probability to be the ratio of the total number of F atoms which form Si−F bonds with the surface to the total number of F atoms which impinge on the surface. For example, if every trajectory at a given initial condition were to result in atom abstraction, the adsorption probability would be 0.5 because one Si−F bond would be formed for each two F atoms (initially in the form of F_2) that arrive at the surface. Overall, the qualitative agreement between our simulations and experimental results is excellent. Both experiment and theory suggest a trend of increasing adsorption probability with increasing F_2 translational energy, as found by both Ceyer and co-workers[13] and Behringer et al.,[15] and the experimental values for S_0 bracket our predictions. Given the disparity between the four sets of experimental data, our simulations are also in reasonable quantitative agreement with the experimental values for S_0. We now discuss, in turn, interactions of F_2 (with varying amounts of incident energy) with Si(100) surfaces covered with zero fluorine atoms (Θ_F = 0 ML), half a monolayer of fluorine atoms (Θ_F = 0.5 ML), and one monolayer of fluorine atoms (Θ_F = 1.0 ML).

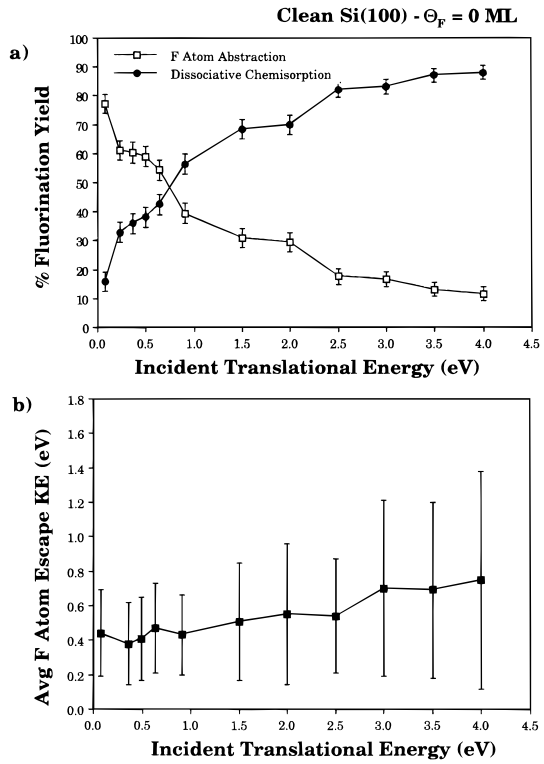

Figure 3. (a) Reaction channel partitioning for F_2 molecules impinging on the clean Si(100)-2×1 surface. The percentage occurrence of each channel is shown as a function of incident translational kinetic energy of the F_2 molecule. (b) Average escape kinetic energy of F atoms ejected from the clean Si(100) surface as a function of the incident translational kinetic energy of the impinging F_2 molecule. The same convention is used in all analogous plots.

III.A. Clean Surface Results (Θ_F = 0 ML). In this section we expand on our previous simulations[24] of F_2 molecules impinging on the clean surface to cover incident COM translational kinetic energies ranging from 0.078 to 4.0 eV for the F_2 molecules. After proposing a mechanism for the reaction of F_2 with the Si(100)-2×1 surface, we will show why this mechanism leads to the results found in our simulations. This detailed analysis of the mechanism will also provide a base line for analyzing our other simulations of F_2 impinging on surfaces with nonzero coverages of adsorbed fluorine atoms.

The actual reaction mechanism can be elucidated to some degree from the relative availability of the possible reaction pathways. Figure 3a shows the percentage occurrence of each reaction pathway for F_2 molecules incident on the clean Si-(100) surface with COM translational kinetic energies ranging from 0.078 to 4.0 eV. Three features are readily apparent in this graph: (i) the nonreactive scattering pathway is unavailable on the clean surface, (ii) abstraction is the dominant trajectory at low incident energies, and (iii) increasing the COM kinetic energy of the incoming F_2 enhances dissociative chemisorption for all incident energies. Each of these features is important in characterizing the reaction dynamics of F_2 interacting with the Si(100) surface.

Let us begin with the absence of nonreactive scattering. In the 2400 trajectories we performed to generate the data in Figure 3a, nonreactive scattering occurred only once, at the lowest F_2 incident energy (0.078 eV). This shows that there is effectively no barrier to reaction for F_2 on the Si(100) surface within our simulations, as basically every F_2 which impinges on the surface results in the formation of a Si−F bond. This is similar to the

result reported by Weakliem et al. for the adsorption of atomic fluorine on the clean Si(100) surface.[23] Using the same interaction potential, their simulations of atomic fluorine impinging on the clean silicon surface yielded $S_0 = 1.0$, regardless of the incident energy of the F atom. These results are in excellent qualitative agreement with the measurements of Li et al.,[13] who observed a negligible amount of scattered F_2 for clean Si(100) surfaces ($\Theta_F = 0$ ML). This is also consistent with data from Behringer et al. and Jensen et al., who reported that adsorption of F_2 molecules on the clean surface was a direct process that did not involve a precursor state.[14,43]

The high percentage of atom abstraction events at low incident energies requires a more detailed analysis. Although atom abstraction is an unusual pathway for reactive scattering of diatomic molecules from surfaces, a combination of factors make abstraction probable. The most significant factor is the large disparity between the bond energy of an F−F bond in an F_2 molecule and an Si−F bond on the silicon surface. The strength of the F−F bond in an F_2 molecule is ∼1.6 eV,[44] while the bond strength of an Si−F bond on the Si(100) surface is ∼6.4 eV.[20] This means that formation of an Si−F bond at the expense of the F−F bond is highly exothermic, and thus it is not necessary for both F atoms in the F_2 molecule to form Si−F bonds for the reaction to be extremely favorable.

The geometry of the surface also contributes to the availability of atom abstraction. The bond length in an F_2 molecule is much shorter than the distance between any neighboring Si atoms on the (100) surface. [R_e(F−F) ∼ 1.4 Å, while R_e(Si−Si) ∼ 2.4, 3.8, or 5.5 Å for the nearest Si atoms in the same dimer, in adjacent dimers in the same row, or in adjacent rows, respectively, as shown in Figure 1a.] As a result, it is difficult for an incoming F_2 molecule to align itself with the surface such that both F atoms in the F_2 can simultaneously form Si−F bonds.

The favorability of forming an Si−F bond at the expense of the F−F bond, combined with the poor geometric matchup of the F_2 molecule with the Si(100) surface, leads us to predict that the reaction of F_2 with the Si(100)-2×1 surface occurs in a stepwise manner. For both F atom abstraction and dissociative chemisorption, the reaction begins with the formation of an Si−F bond at one of the dangling bond sites on the surface, yielding an Si−F−F complex. This complex falls apart via release of the F atom which is not participating in the Si−F bond. Once the second F atom is released from the Si−F−F complex, then, depending on its momentum, this atom can either leave the surface, yielding an F atom abstraction event, or form another Si−F bond on the surface, leading to dissociative chemisorption. While a concerted reaction where two Si−F bonds from roughly simultaneously is still possible, we found that this occurs in a minuscule number of trajectories within our simulations. The direction of motion of this ejected fluorine determines whether the trajectory results in atom abstraction or dissociative chemisorption. If the velocity of the ejected F atom is primarily parallel to the surface, then the F atom will have an opportunity to find a second dangling bond site and form a second Si−F bond. As mentioned above, simulations of F atoms impinging on the clean Si(100) surface show no barrier to reactivity, so any F atom which comes into close proximity to a dangling bond site should form an Si−F bond. As a result, an F atom diffusing along the surface will react with the first dangling bond site it encounters along its flight path. This suggests that diffusion should be limited on the surface, and accordingly our simulations indicate that dissociative chemisorption trajectories usually involve formation of Si−F bonds at neighboring sites on the surface for all of the F_2 incident energies we studied. A similar result has been observed by Jensen et al. for F_2 molecules undergoing dissociative chemisorption on the Si(111)-7×7 surface.[45] The lack of dependence on incident energy is due to the very deep (∼6 eV) Si−F well encountered by the F atoms, which renders it unlikely that incident energies below 6 eV would show an adsite dependence. On the other hand, if the velocity of the ejected F atom is directed primarily along the surface normal, then the F atom will leave the interaction range of the surface before it has an opportunity to find a second dangling bond site.

Although this mechahism can easily account for the presence of abstraction trajectories, the high probability of abstraction at low energies and the increase in dissociative chemisorption at higher energies still require explanation. We note that our prediction of the dominance of F atom abstraction by silicon surfaces at low F_2 incident energies with increasing amounts of dissociative chemisorption as the incident energies increase has been confirmed via scanning tunneling microscopy by Jensen, Yan, and Kummel for F_2 molecules impinging on the Si(111) surface.[43] Figure 3b shows the average exit energies for F atoms ejected during atom abstraction as a function of increasing incident F_2 COM translational energy. Immediately obvious from this graph is the hyperthermal character of the ejected F atoms, a qualitative feature which has also been observed experimentally by Li et al.[12] Even the lowest F_2 incident energy, 0.078 eV, results in an average exit energy for ejected F atoms of 0.4 eV, as compared to the 0.03 eV expected for the average energy of an atom at 298 K, the surface temperature. Clearly the ejected F atoms have not equilibrated with the surface. On the other hand, the escaping F atoms have little memory of their initial conditions, as increasing the incident F_2 energy from 0.078 to 4.0 eV results in a change in the average exit energy from 0.4 eV to only 0.8 eV. The fact that the F atoms are not equilibrated with the surface yet have kinetic energies only weakly correlated with their initial conditions corresponds to F atoms which are "chattering" at the reaction site. In other words, during the stepwise reaction mechanism we are proposing, when an Si−F bond is formed by an incoming F_2 molecule, the F atom not involved in the Si−F bond is not immediately released. It spends enough time in an Si−F−F complex state to lose most of its memory about the initial F_2 state, but not long enough to be chemisorbed and hence equilibrated to the surface temperature. As a result, the hyperthermal exit energies are probably mostly indicative of repulsions in the Si−F−F potential. These repulsions arise from the sudden switching of potential energy surfaces, from an attractive F−F potential, prior to reaction, to a repulsive Si−F−F potential postreaction. Thus, the ejected F atom suddenly slides down a repulsive potential wall, picking up excess energy as it leaves.

The high exit energies of F atoms ejected from the surface during abstraction provide some insight into the prevalence of this reaction pathway at low F_2 incident energies. Clearly F atoms ejected from the Si−F−F complexes possess enough translational kinetic energy to escape weak interactions with the surface. However, a full understanding of the large number of abstraction events requires examination of the angular distribution of the ejected F atoms. Figure 4a shows the angular distribution relative to the surface normal of F atoms produced by abstraction on the clean Si(100) surface for F_2 molecules with 0.078 eV of incident translational energy. In this plot, an exit angle of 0° represents exit along the surface normal, while a 90° exit angle would lie in the plane of the surface. The exit angles have been placed in bins of 5°, so the point at 10° represents the relative number of F atoms which had exit angles between 10° and 15°. The dominant feature in this graph is

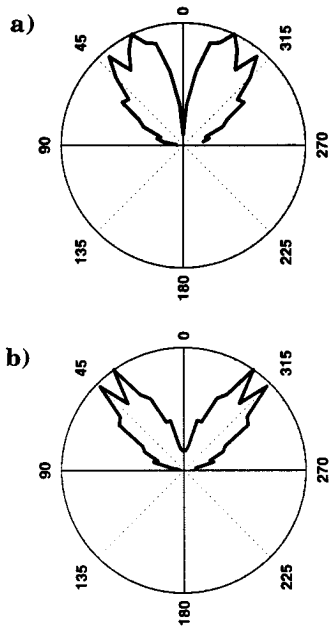

Figure 4. Angular distribution relative to the surface normal of F atoms ejected during abstraction events for F_2 molecules impinging on the clean Si(100) surface with (a) 0.078 eV and (b) 0.642 eV of incident translational kinetic energy. 0° is aligned with the surface normal, while 90° is in the plane of the surface. The same convention is used in all analogous plots.

the location of the peak intensity at the bin containing exit angles between 25° and 30°. Although the distribution is broad, it is clearly centered around this angle. Two satellite peaks are also present 10° away on each side of the main peak.

We believe that this distribution can be explained by breaking it down into two main components. The main peak at 25°−30° is due to the majority of trajectories where the second F atom is ejected promptly after Si−F bond formation, representing the desire of the F_2 bond axis to align with the Si−F bond axis during Si−F bond formation at a dangling bond site. The satellite peaks are a result of the minority of trajectories where the Si−F−F complex lasts for more than one oscillation. In a classical oscillator, the oscillator spends its greatest amount of time near the turning points of the oscillation, as the velocity of the oscillator is lowest near the turning point. The satellite peaks correspond to ejection of the second F atom along the F−F bond axis when the Si−F−F complex is at or near the turning point. This is in coincidental agreement with experimental results from electron-stimulated desorption ion angular distribution measurements.[34−36] ESDIAD actually measures the Si−Si−F angle, while our result is for an F atom released from an Si−F−F complex. Experimental values for the angle an Si−F bond makes with the surface normal indicate an angle of 29°−36°, consistent with our prediction for the F atom ejection angle. Based on the angular distribution in Figure 4a, most of the F atoms released after an F_2 forms an Si−F bond will not stay near the surface long enough to find a second dangling bond site, thus leading to a high percentage of abstraction events at low F_2 incident energies.

While Figure 4a provides an explanation for the initially high levels of abstraction found in our simulations, examination of additional exit angle distributions may provide insight into the decrease in abstraction at higher F_2 incident energies. Figure 4b shows the same type of angular distribution plot; only this time the F_2 incident energy is 0.642 eV. Once again, the angular distribution is broad, with lower intensity satellite peaks on either side of the main peak. However, the main peak is now at 35°−40° from the surface normal, as opposed to the 25°−30° value for an F_2 incident energy of 0.078 eV. Figure 4b shows that increasing the incident energy of the incoming F_2 molecule leads to a depression of the F atom ejection angle away from the surface normal. This is simply due to increased penetration of the surface as a result of the higher incident F_2 energy, which results in F atoms scattering at larger angles. With exit angles which are farther from the surface normal, the ejected F atoms spend more time within the interaction range of the surface. This increases the likelihood of the F atom finding a second dangling bond site and leads to increased dissociative chemisorption at the expense of atom abstraction, as seen in Figure 3a. Note that the depression of exit angle toward the surface in Figure 4b takes place in spite of the fact that F atoms with exit angles closer to the surface have a higher probability of being captured by a nearby dangling bond site. One might expect that the increased capture rate of F atoms with ejection angles closer to the surface would push the exit angular distribution toward the surface normal, mitigating the exit angle depression caused by increased F_2 incident energy. However, we see that, of those F atoms that do escape, many are still escaping at large exit angles.

We now have a full picture of the generic reaction mechanism for F_2 molecules impinging on the Si(100)-2×1 surface. As F_2 approaches the Si surface, typically one of the F atoms in the incoming molecule is strongly attracted to a dangling bond site on the surface. An Si−F bond forms, followed closely by the ejection of the second F atom. For low-incident energy F_2 molecules, the ejected F atom is most likely to escape from the surface due to a combination of an average exit angle of 30° from the surface normal (along the Si−F bond axis direction) and a hyperthermal escape velocity resulting from the overall reaction exothermicity and the sudden switch from an attractive to a repulsive potential surface. As the energy of the incident F_2 molecule increases, the escape velocity of ejected F atoms increases slowly. This slight increase in escape energy is more than compensated for by a depression of the exit angle for ejected F atoms, leading to ever increasing amounts of dissociative chemisorption as the incident energy is increased.

III.B. $\Theta_F = 0.5$ ML Surface Results. The reaction of F_2 molecules with the clean Si(100)-2×1 surface represents the simplest system we will investigate. Having deduced a detailed reaction mechanism for F_2 molecules impinging on the clean surface, we can use this mechanism as a guide for interpreting results on surfaces which have fluorine atoms already adsorbed on the surface.

As described in section II, the $\Theta_F = 0.5$ ML partially fluorinated surface used in these simulations was created by fluorinating one dangling bond per silicon surface dimer. This was done without disrupting the underlying dimer row structure of the silicon surface, so the net result is a surface where half of the dangling bond sites are now occupied by fluorine atoms making Si−F bonds. Figure 5 shows a schematic representation of a small portion of a silicon surface fluorinated in this manner.

The most obvious difference in the reactivity of F_2 impinging on the $\Theta_F = 0.5$ ML partially fluorinated surface as compared to the clean surface is the availability of the nonreactive scattering pathway. This can be seen in Figure 6a, which shows the probability of occurrence of each reaction pathway for the $\Theta_F = 0.5$ ML partially fluorinated surface over the same range of F_2 incident energies displayed in Figure 3a. Nonreactive scattering occurs 42 ± 5% of the time at the lowest incident energy. This value decreases with increasing incident energy but is still above 10% even at 4 eV. The percentage occurrence of atom abstraction is also markedly different. Although it is initially less probable for the $\Theta_F = 0.5$ ML surface as compared

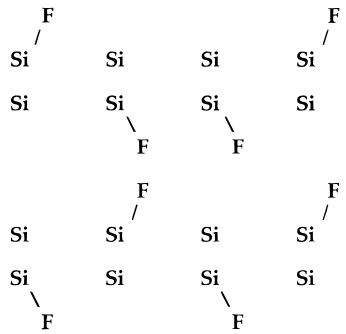

Figure 5. Schematic of a portion of a $\Theta_F = 0.5$ ML surface. Half of the Si atoms on the surface are participating in Si−F bonds, with exactly one Si−F group per dimer. The F atoms are randomly distributed in each dimer.

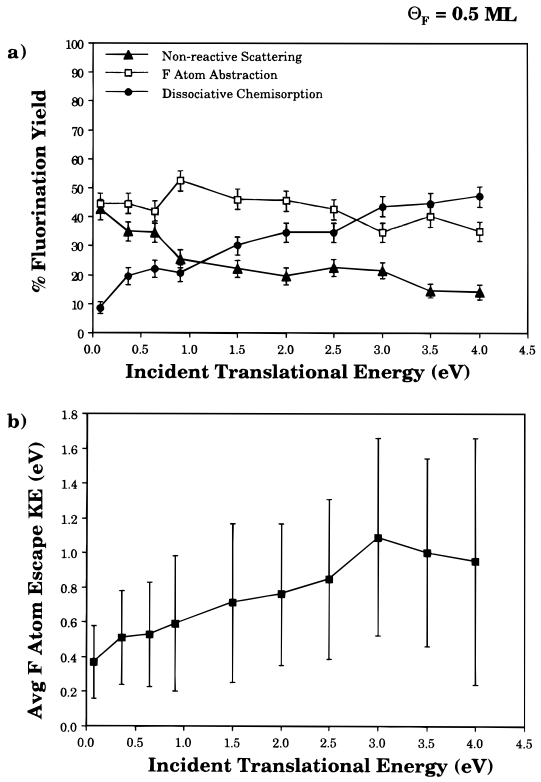

Figure 6. (a) Reaction channel partitioning for F_2 molecules impinging on the $\Theta_F = 0.5$ ML surface and (b) average escape energy of F atoms ejected from the $\Theta_F = 0.5$ ML surface as a function of the incident translational kinetic energy of the impinging F_2 molecule. See Figure 3 for a full description.

to the clean surface, the amount of abstraction stays relative constant regardless of incident energy, causing abstraction to be more likely on the $\Theta_F = 0.5$ ML surface than on the clean surface at energies above 1.0 eV. This is in qualitative agreement with the experimental results of Li et al.,[12] who reported a maximum in the number of atom abstraction events at a nonzero coverage. The dissociative chemisorption pathway appears to have changed at least. On the $\Theta_F = 0.5$ ML surface, it once again starts out with a low probability of occurrence that increases with the incident energy of the impinging F_2 molecule. The change in dissociative chemisorption as incident energy increases is more dramatic on the clean surface, but the qualitative behavior is similar.

The introduction of nonreactive scattering and its decrease with incident energy is the easiest pathway to explain. Since half of the dangling bond sites on the surface are occupied by a fluorine atom bonded to the surface, it follows that half of the fluorine molecules which impinge on the surface in our simulations will be closer to an occupied site than an unoccupied site. As these molecules approach the surface, they will encounter a primarily repulsive interaction with the surface Si−F group first. The percentage of incident molecules undergoing nonreactive scattering at the lowest incident energy simulated, $42 \pm 5\%$, is close to the 50% of molecules which approach the surface closer to an occupied dangling bond site. Thus, the majority of F_2 molecules which approach the surface above an occupied dangling bond site are scattered from the surface, consistent with Langmuirian kinetics, where the probability for scattering would be expected to grow linearly with coverage.

As the incident energy of the F_2 is increased, greater repulsions are required to reverse the momentum of the incoming molecule. This will not make a great deal of difference for molecules which land on the surface directly above an Si−F group, as these will still scatter. However, for F_2 molecules which approach near to an Si−F group instead of directly above, the higher incident energy gives the F_2 a greater chance to glance off of the Si−F bond. If the F_2 molecule is repelled by the Si−F group in such a way that the velocity of the F_2 molecule is primarily parallel to the surface, the F_2 molecule may be able to diffuse on the surface and find an unoccupied dangling bond site to react with.

Since nonreactive scattering is present for all F_2 incident energies on the $\Theta_F = 0.5$ ML surface, clearly the amounts of atom abstraction and dissociative chemisorption will be reduced. The 30%−40% of nonreactive scattering present at low incident energies can somewhat account for the lower abstraction and dissociative chemisorption percentages. However, this new reaction channel cannot explain the relative changes between abstraction and dissociative chemisorption. For example, on the clean surface, dissociative chemisorption surpasses atom abstraction as the dominant trajectory at 0.75 eV of incident energy in the incoming F_2 molecules, as shown in Figure 3a. By contrast, Figure 6a shows that, for the $\Theta_F = 0.5$ ML surface, dissociative chemisorption only becomes more probable than abstraction for F_2 incident energies greater than 2.75 eV. This shows that the relative amount of dissociative chemisorption has decreased as compared to abstraction.

The movement of the crossover point to higher incident energies is also an effect of the preadsorbed fluorine. In our stepwise reaction mechanism, dissociative chemisorption occurs when the second F atom stays close enough to the surface to find another dangling bond site. With half of the dangling bond sites already occupied on the $\Theta_F = 0.5$ ML surface, some F atoms ejected from an Si−F−F complex which stay close to the surface long enough to find another dangling bond site will now encounter an Si−F group. These F atoms will be unable to form Si−F bonds and may scatter away from the surface, leading to additional abstraction events at the expense of dissociative chemisorption. This decrease in dissociative chemisorption relative to atom abstraction results in the increased F_2 incident energy necessary for dissociative chemisorption to become the dominant outcome.

We are now in a position to better understand the apparent lack of influence of increasing incident energy on atom abstraction. Although increasing the F_2 incident energy enhances dissociative chemisorption at the expense of atom abstraction, this effect is mitigated on the $\Theta_F = 0.5$ ML surface by the site blocking mechanism just described. On the basis of this alone, we would still expect atom abstraction to decrease at higher incident energies. However, increasing incident energy also leads to a reduction in nonreactive scattering. This increases the total number of abstraction plus dissociative chemisorption events or reactive events. Thus, although the

TABLE 2: Comparison of Adsorption Probabilities

F_2 incident energy (eV)	S_0[a]	$S_{0.5}$[b]	F_2 incident energy (eV)	S_0[a]	$S_{0.5}$[b]
0.078	0.55 ± 0.03	0.31 ± 0.03	2.000	0.85 ± 0.04	0.57 ± 0.05
0.364	0.66 ± 0.03	0.42 ± 0.04	2.500	0.91 ± 0.02	0.56 ± 0.04
0.642	0.70 ± 0.05	0.43 ± 0.05	3.000	0.91 ± 0.02	0.61 ± 0.02
0.906	0.76 ± 0.04	0.47 ± 0.04	3.500	0.94 ± 0.02	0.65 ± 0.03
1.500	0.84 ± 0.02	0.53 ± 0.04	4.000	0.94 ± 0.02	0.65 ± 0.04

[a] S_0 = adsorption probability on the clean Si(100) surface. [b] $S_{0.5}$ = adsorption probability on the $\Theta_F = 0.5$ ML surface.

relative number of abstraction events decreases due to enhancement of the dissociative chemisorption pathway as the F_2 incident energy increases, the total number of reactive events also increases, leading to little or no change in the absolute number of abstraction events.

In order to facilitate a more quantitative comparison of the reactivities, we can compute the adsorption probability for each initial condition on each surface. Table 2 lists the F_2 adsorption probability, as defined at the beginning of section III, at selected F_2 incident energies for the two surfaces considered thus far. Comparing the values in the second and third columns, showing the clean and $\Theta_F = 0.5$ ML surfaces, respectively, demonstrates that the adsorption probability on the $\Theta_F = 0.5$ ML surface is significantly decreased compared to the adsorption probability on the clean surface at all incident energies.

To this point we have only demonstrated that the mechanism found for reaction of F_2 with the clean Si(100) surface is consistent with the results found on a surface with 0.5 ML of fluorine atoms. Further evidence that the same mechanisms apply to both reactions can be found by once again examining the exit characteristics of F atoms ejected during abstraction events. Figure 6b shows the translational kinetic energy for F atoms produced during abstraction events for the $\Theta_F = 0.5$ ML surface. Overall, the exit energies for ejected F atoms are similar for the clean and $\Theta_F = 0.5$ ML surfaces, as the escaping F atoms have on average roughly the same energy for both surfaces, as well as having roughly the same extremely weak dependence on the initial COM translational kinetic energy of the impinging F_2 molecule. The average energy for F atoms ejected from the $\Theta_F = 0.5$ ML surface is slightly higher at all F_2 incident energies, but both surfaces demonstrate broad distributions for all initial conditions and the differences are small relative to the width of these distributions.

We can also consider the angular distribution of the ejected F atoms relative to the surface normal. Figure 7a depicts the distribution for F atoms leaving the surface due to abstraction events for F_2 molecules impinging on the $\Theta_F = 0.5$ ML surface with an incident energy of 0.078 eV. Much like the clean surface, the distribution is broad with very little intensity near 0°, the surface normal. Also, the position of the main peak at 30°−35° away from the surface normal is once again similar to the direction of the Si−F bond axis on the surface. Figure 7b shows the angular distribution for F atoms leaving the surface due to F_2 molecules with 0.642 eV of incident COM translational kinetic energy striking the $\Theta_F = 0.5$ ML surface. Once again, the increase in incident COM translational kinetic energy leads to a depression of the angular distribution away from the surface normal. The higher incident momentum results in the F_2 molecules hitting deeper into the surface before reacting, which forces the escaping F atoms to come off at angles farther from the surface normal. However, in spite of this effect, the percentage of atoms leaving at angles >45° from the surface normal is still rather small. This is a general trend for F atoms scattered in our simulations, as atoms which are ejected with

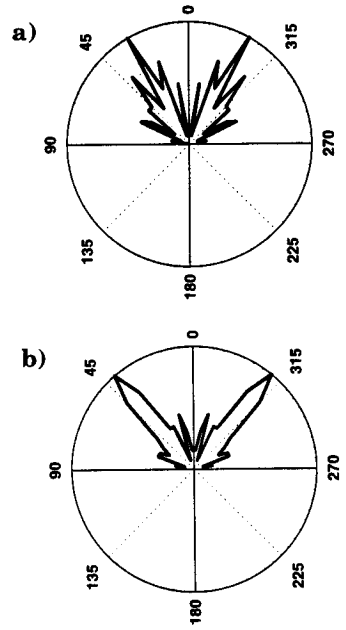

Figure 7. Angular distribution relative to the surface normal of F atoms ejected during abstraction events for F_2 molecules impinging on the $\Theta_F = 0.5$ ML surface with (a) 0.078 eV and (b) 0.642 eV of incident translational kinetic energy. See Figure 4 for a full description.

angles close to grazing either find available dangling bond sites, leading to dissociative chemisorption, or find an occupied dangling bond site and are scattered away at an angle closer to the surface normal by the strong repulsive action of an F atom approaching an Si−F bond too closely. The similarities in the dynamics of the F atoms ejected from both the clean and $\Theta_F = 0.5$ ML surfaces suggest that atom abstraction events on both surfaces are occurring by the same mechanism.

III.C. $\Theta_F = 1$ ML Surface Results. On the basis of the expected Langmuirian $1 - \Theta_F$ dependence for the reactivity of the $\Theta_F = 0.5$ ML surface toward incident F_2, one would expect the adsorption probability for the $\Theta_F = 1$ ML ordered surface to be close to zero. Our simulations concur with this prediction, as shown in Figure 8a. Most notable in Figure 8a is the absence of data points below 2.5 eV of COM translational kinetic energy. This is due to a barrier to reaction for F_2 impinging on a $\Theta_F = 1$ ML ordered surface, which our simulations predict to be between 2.0 and 2.25 eV. For incident energies of 2.5 eV and greater, the only Si−F bond formation is due to atom abstraction, as dissociative chemisorption does not occur. An additional nonreactive pathway is also available in the form of collision-induced dissociation of F_2.

The reactivity of the $\Theta_F = 1$ ML ordered surface provides further information about the reactivity of F_2 toward Si(100) surfaces with preexisting fluorine coverage. The stepwise mechanism we have proposed is based on the first Si−F bond forming at an unoccupied dangling bond site. The fact that reaction can take place in the absence of dangling bonds for incident translational kinetic energies above 2.25 eV implies a new mechanism is occurring. Our simulations indicate that large translational kinetic energies allow F_2 molecules to fight past the layer of Si−F species and attack Si atoms in the second layer. This attack occurs in the channels in between the dimer rows. Notably, none of the reactions occur with first layer Si atoms, which already have one Si−F bond. This would create SiF_2 species on the surface, but this type of reaction was not observed in our simulations. Attack of these first layer atoms might initially appear more favorable than reaction with second layer atoms, due to the lower strength Si−Si dimer bond of the first layer atoms. However, the barrier to attacking the first

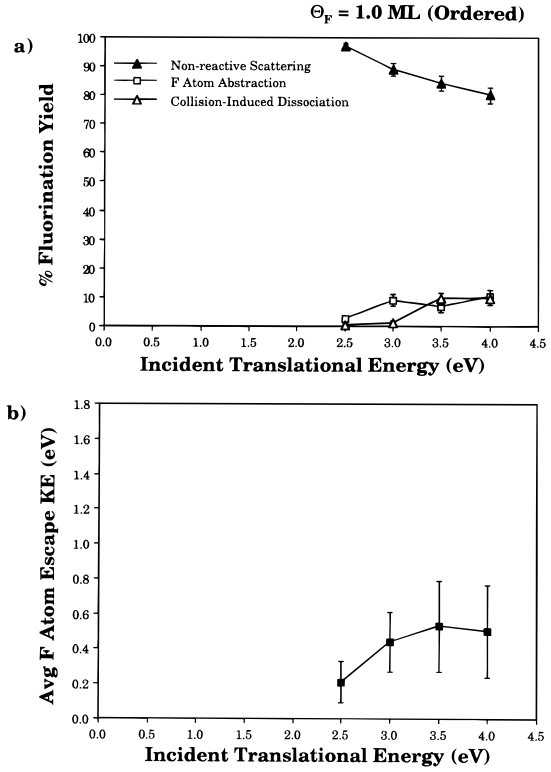

Figure 8. (a) Reaction channel partitioning for F_2 molecules impinging on the $\Theta_F = 1.0$ ML ordered surface and (b) average escape energy of F atoms ejected from the $\Theta_F = 1.0$ ML ordered surface as a function of the incident translational kinetic energy of the impinging F_2 molecule. See Figure 3 for a full description.

layer atoms, which are already participating in one Si−F bond, is much higher in our simulations than forming a bond to a subsurface Si atom which is only bonded to other Si atoms. This is due to large nonbonded repulsions between the incoming and adsorbed F atoms. (Additional calculations show that energies of greater than 5.0 eV are necessary to cause F_2 molecules to react with the first layer Si−F groups to form an SiF_2 group on the surface.[46])

Although Si−F bonds formed on the $\Theta_F = 1$ ML ordered surface occur via an activated process instead of the barrierless attack at an available dangling bond site, the reaction mechanism is otherwise the same as found on the clean surface. Figure 8b shows the average exit energy for F atoms ejected during abstraction events from this surface. The same type of broad distribution of hyperthermal exit energies found for the clean and $\Theta_F = 0.5$ ML surfaces is also predicted for the $\Theta_F = 1$ ML ordered surface. The absence of dissociative chemisorption events is also in agreement with the proposed reaction mechanism, as no unoccupied surface dangling bond sites are available for reaction, leading to atom abstraction as the only available pathway yielding Si−F bond formation.

The $\Theta_F = 1$ ML ordered surface exhibits almost no reactivity toward incident F_2 molecules, but other structures of 1 ML surfaces may be more reactive. Previously, Weakliem et al. studied the interaction of F atoms with the Si(100) surface using high incident fluxes.[22,23] They found that a $\Theta_F = 1$ ML ordered surface is basically unreactive for low-incident energy F atoms, similar to our finding for F_2. However, when they started the simulation with a clean surface and allowed the fluorosilyl layer to grow during the simulation, they observed disruption of the surface layer, leading to exposure of dangling bonds from lower layer atoms. This allowed uptake of more than 1 ML of fluorine by the surface, in contrast to the results for the ordered surface. As a result, they concluded that surface disorder was critical to real etching reactions, as some means for regenerating surface dangling bonds is necessary to sustain the reaction.

On the basis of these results, we created a $\Theta_F = 1$ ML disordered surface to contrast its reactivity to that of the $\Theta_F = 1$ ML ordered surface. In order to build this surface, we used the same base slab of nine silicon layers each containing 64 atoms. We forced the initially clean surface to reconstruct into the experimentally observed p(2×1) pattern and equilibrated the surface to 298 K. We then added fluorine atoms to the simulation, each having 1.5 eV of translational kinetic energy. The initial velocity of each F atom was directed normal to the surface. Each F atom was initially placed at a random location above the surface at a fixed height beyond the interaction range of any surface atoms. We propagated our simulation forward in time using a split simulation cell. The upper four layers of our silicon slab, as well as any fluorine atoms, were propagated using a Verlet algorithm for microcanonical (NVE) dynamics. Again, this is the ensemble which mimics the actual dynamics of a system. However, the creation of more than a few Si−F bonds in a system of this size could cause an unrealistic heating of our crystal because of the tremendous exothermicity of this reaction. Thus, we used canonical isothermal (NVT; constant number of particles, volume, and temperature) dynamics to propagate the remaining moving layers of the silicon slab. This allows us to retain the correct dynamics for the upper layers, where all reactions are occurring, while dissipating excess heat in the lower layers, as a real crystal would. (As mentioned in the simulation details, the bottom layer of the slab remains fixed in the ideal bulk position.) The first 10 F atoms were introduced to the surface with random initial positions above the surface and a time interval of 4.5 ps between each F atom to allow time for excess energy to propagate from the upper layers down into the NVT-treated portion of the slab. (Each of these F atoms formed a Si−F bond with the surface.) The next 10 F atoms were added in a slightly different manner. Starting with the surface which already had 10 F atoms adsorbed on it, we ran 10 separate trajectories involving the addition of a 1.5 eV translationally excited F atom, each using a different randomly generated starting position above the surface. We then inspected each trajectory after 4.5 ps of simulation and chose the trajectory which involved the most surface disruption. Using this surface with 11 preadsorbed F atoms, we repeated this procedure. This continued until we generated a surface with 20 preadsorbed F atoms. All remaining F atoms were added to the surface by the same method used for the first 10, consecutively adding 10 F atoms separated in time by 4.5 ps. As the amount of preadsorbed fluorine increased, increasing numbers of F atoms impinging on the surface were scattered away and did not form an Si−F bond. These F atoms were removed from the simulation once they escaped the interaction range of the potential. We continued this scheme until we generated a surface having 64 Si−F bonds. (No silicon atom formed more than one Si−F bond.) Finally, we equilibrated this slab to yield a surface temperature of 298 K. This generated a surface which had small regions of disorder with available dangling bonds (∼10% of the surface), but where the majority of the surface still retained the saturated F−Si−Si−F structure. We denote this as a "disordered" surface even though it really provides only a lower bound for the reactivity of a more disordered surface that appears to form under steady state etching conditions.[5,6,8,9,22,23]

Figure 9a shows the reaction channel partitioning for the interaction of F_2 with a $\Theta_F = 1$ ML "disordered" surface. The most obvious feature is the lower energy required to achieve Si−F bond formation, as is evident from the presence of both

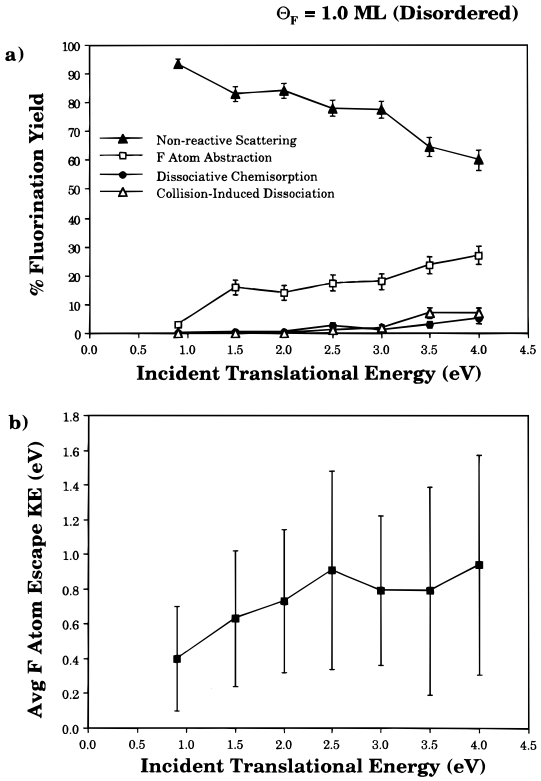

Figure 9. (a) Reaction channel partitioning for F_2 molecules impinging on the $\Theta_F = 1.0$ ML disordered and (b) average escape energy of F atoms ejected from the $\Theta_F = 1.0$ ML disordered surface as a function of the incident translational kinetic energy of the impinging F_2 molecule. See Figure 3 for a full description.

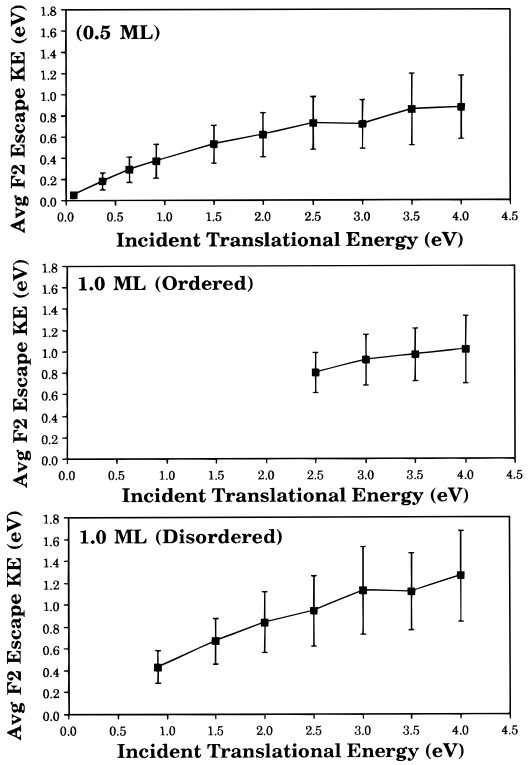

Figure 10. Average escape kinetic energy for F_2 molecules undergoing nonreactive scattering as a function of the incident F_2 translational kinetic energy for the (a) $\Theta_F = 0.5$ ML surface, (b) $\Theta_F = 1.0$ ML ordered surface, and (c) $\Theta_F = 1.0$ ML disordered surface.

atom abstraction and dissociative chemisorption at 0.906 eV, the lowest energy simulated. In fact, based on our simulations, there is probably no barrier to reaction for this surface. This is due entirely to the regions of the surface where dangling bonds are already exposed. For incident F_2 COM translational energies below ~2 eV, all atom abstraction and dissociative chemisorption events occur at these dangling bond sites. Reaction with other portions of the surface still requires overcoming a reaction barrier and thus only occurs at much higher energies. This also accounts for why we did not investigate lower incident energies, as below 0.906 eV the only reactivity was due to those F_2 molecules which approached the surface directly above one of the few unoccupied dangling bond sites.

In spite of the absence of a barrier, qualitatively the reactivity of the $\Theta_F = 1$ ML disordered surface is similar to that of the ordered surface. Nonreactive scattering still dominates for all incident energies, with increasing COM translational energy primarily enhancing atom abstraction at the expense of nonreactive scattering. The small number of dissociative chemisorption events observed occur exclusively at those sites on the surface where two unoccupied dangling bond sites are in close proximity to each other.

As might be expected, the average exit energies for F atoms ejected during abstraction from the $\Theta_F = 1$ ML disordered surface are roughly the same as those found on the other surfaces. Figure 9b shows the average F atom exit energy for the $\Theta_F = 1$ ML disordered surface. Once again, this graph shows the broad, hyperthermal distribution of exit energies seen for all of the other surfaces we studied that are only weakly dependent on the F_2 initial conditions.

III.D. Inelastic Scattering of F_2. To this point, we have examined in detail the partitioning between reaction channels for F_2 reacting with various Si(100) surfaces, as well as some of the characteristics of the dissociative chemisorption and atom abstraction pathways as they relate to the reaction mechanism. By contrast, we have touched only briefly on the nonreactive scattering pathway. Just as for F atoms ejected during abstraction, we can gain a better understanding of the nonreactive scattering pathway by examining the the characteristics of the scattered F_2 molecules.

Figure 10a−c shows the average kinetic energy of F_2 molecules scattering from the $\Theta_F = 0.5$ ML, 1 ML ordered, and 1 ML disordered surfaces. We will focus first on Figure 10a, as we have the widest range of incident F_2 energies for the $\Theta_F = 0.5$ ML surface. Figure 10a shows that nonreactive scattering of F_2 molecules from the $\Theta_F = 0.5$ ML surface is a highly inelastic process. The exit energies of the F_2 molecules are up to ~4 times smaller than the incident energies for all initial conditions studied, although the exit energy of the F_2 molecules does have a moderate dependence on the incident F_2 translational kinetic energy. This dependence on the incident energy clearly shows that the scattered F_2 molecules do not equilibrate with the surface temperature before they leave interaction range of the surface. Rather, the F_2 molecules scatter away directly upon impact, although with ~50−75% less than their incident energy. These same trends are also visible in Figure 10, b and c, for the $\Theta_F = 1$ ML ordered and disordered surfaces, respectively.

Unlike the ejected F atoms, scattered F_2 molecules can also be vibrationally excited as they leave the surface. Clearly, some amount of the F_2 incident translational energy is transferred to vibration upon scattering, as collision-induced dissociation becomes an available pathway for high-incident energy F_2 molecules impinging on the $\Theta_F = 1$ ML surfaces. Figure 11 quantifies this transfer for F_2 molecules scattered off of the $\Theta_F = 1$ ML disordered surface by displaying the average vibrational energy of the scattered F_2 molecules for each F_2 incident kinetic energy. The vibrational energy for the scattered F_2 molecules

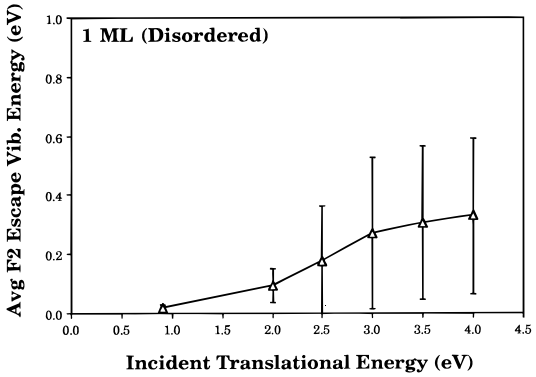

Figure 11. Vibrational energy of F_2 molecules undergoing nonreactive scattering from the $\Theta_F = 1.0$ ML disordered surface as a function of the incident F_2 translational kinetic energy.

was calculated by collecting the length of the F−F bond at each time step for the F_2 molecules. The largest separation of the two F atoms after leaving the interaction range of the surface was chosen as the classical turning point for the vibration. The F−F bond energy was calculated for this distance and subtracted from the value of the F−F bond energy at the equilibrium bond distance in the SW potential (1.435 Å) to determine the (classical) vibrational energy. (For reference, one vibrational quantum for F_2 is 0.114 eV.[44]) The amount of vibrational energy transferred into the F−F bond during nonreactive scattering exhibits primarily a linear dependence on the F_2 incident energy, although this dependence tails off somewhat above 2.5 eV as the most highly vibrationally excited F_2 molecules undergo collision-induced dissociation.

The raises a question we have yet to address, namely, the influence of vibrational energy of F_2 molecules on reactivity. In our previous work, we investigated the influence of up to ∼1 eV of vibrational energy in the F−F bond on reactivity toward the clean Si(100) surface.[24] In these simulations, the incident COM translational kinetic energy of the F_2 molecule was held constant at our lowest value of 0.078 eV. In Figure 12a, which shows the reaction channel partitioning in these simulations, the total energy is displayed along the abscissa, so the vibrational excitation for each point is equal to the total energy minus 0.078 eV. These results show that vibrational energy is moderately effective for increasing reactivity for vibrational energies up to ∼0.5 eV, but plateaus beyond that point. We performed an additional limited study of the influence of vibrational energy on reactivity with the $\Theta_F = 0.5$ ML surface. Figure 12b contains data for only four incident energies, but it is already evident that increasing vibrational excitation is having little or no effect on the F_2 reactivity, aside from enhancing the abstraction pathway. This is to be expected, since the F atom which does not form the first Si−F bond has increased (vibrational) kinetic energy, which increases the probability that it will escape the surface. Since abstraction is not expected to be as effective as dissociative chemisorption in terms of increasing etching, we conclude that vibrational excitation of the F_2 molecule has only limited ability to enhance reactivity.

There is a second consequence to the transfer of vibrational energy into the F−F bond upon collision with the Si(100) surface. We predict that for both the $\Theta_F = 1$ ML ordered and disordered surfaces that collision-induced dissociation starts occurring at ∼2.5 eV. We have also shown that the average vibrational energy of scattered F_2 molecules continues to rise with increasing F_2 incident translational energy. One possible consequence of this trend is that further translational excitation of incident F_2 molecules could eventually lead to collision-induced dissociation as the primary reaction channel on surfaces with high fluorine coverage, as the impinging F_2 molecule would fall apart immediately upon impact, instead of penetrating the initial fluorine layer to find a reactive site. We are investigating this further.[46]

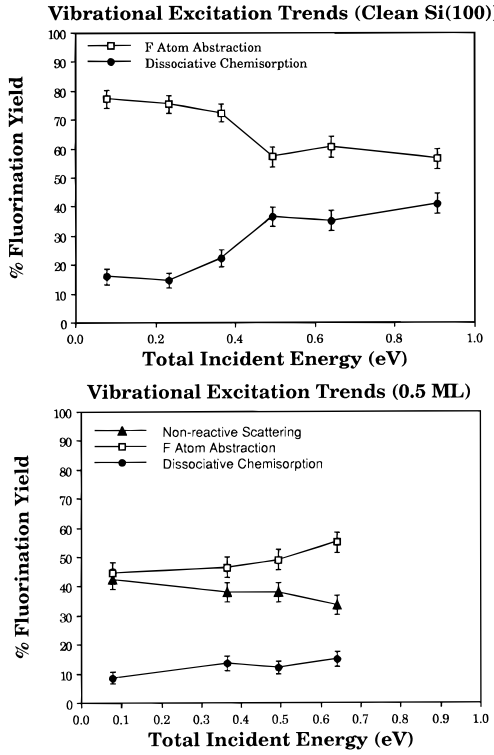

Figure 12. Reaction channel partitioning for F_2 molecules impinging on (a) the clean Si(100) surface and (b) the $\Theta_F = 0.5$ ML surface. The percentage occurrence of each channel is shown as a function of the incident translational kinetic energy plus vibrational energy of the F_2 molecule.

We can also characterize the angular distribution of the scattered F_2 molecules. Figure 13a shows the angular distribution for F_2 molecules with incident kinetic energy of 0.078 eV that were scattered away from the $\Theta_F = 0.5$ ML surface. The distribution of exit angles is broad and lacks a distinct maximum, although the number of molecules scattered directly back along the surface normal is low, suggesting again that the corrugated nature of this surface precludes scattering along the surface normal. Figure 13b, depicting the distribution of scattered F_2 molecules with incident translational kinetic energies of 0.642 eV, contains a similarly broad distribution. As was the case for ejected F atoms, increasing the incident kinetic energy of the incoming F_2 molecules leads to a depression of the angular distribution of scattered F_2 molecules away from the surface normal. However, unlike the case for ejected F atoms, this trend eventually reverses itself. Figure 13c once again shows an angular distribution for F_2 molecules scattered from the $\Theta_F = 0.5$ ML surface, but this time the incident translational kinetic energy is 3.0 eV. The characteristics of the distribution have now changed in several ways. First, the distribution has narrowed, bunching up relatively close to 25° away from the surface normal. It is much closer to the surface normal, although the probability for scattering along the surface normal is still low. Thus, the proximity of the main peak to the surface normal shows that the angular distribution is not continually depressed away from the surface normal by increasing incident translation kinetic energy. This return of the F_2 exit angular distribution toward the surface normal is due to the "apparent" loss of corrugation for the high-incident energy F_2 molecules. As the

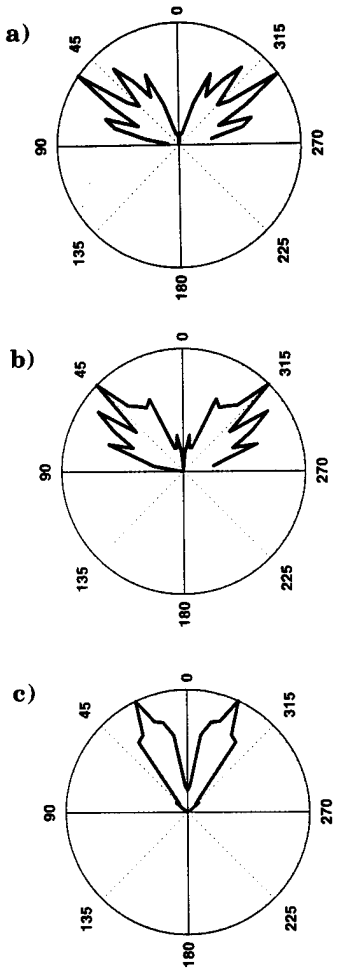

Figure 13. Angular distribution relative to the surface normal of F_2 molecules nonreactively scattered from the $\Theta_F = 0.5$ ML surface with (a) 0.078 eV, (b) 0.642 eV, and (c) 3.0 eV of incident F_2 translational kinetic energy. See Figure 4 for a full description.

energy of the incident F_2 molecule increases, any corrugation in the surface appears to the F_2 to be relatively smaller, causing differences in potential energy that greatly influence a molecule with <1.0 eV of incident energy to have little effect on a molecule with 3.0 eV or more of energy. Thus, the higher energy F_2 molecules effectively feel a flatter potential energy surface than the lower incident energy F_2 molecules.

III.E. Azimuthal Dependence of Scattered F Atoms. Finally, having found a dependence on the local surface geometry in the angular distribution of exiting F atoms relative to the surface normal, we might also expect a dependence in the azimuthal angle. Figure 14 shows the azimuthal angular distribution of F atoms ejected during abstraction on the clean surface for incident F_2 energies of 0.078 and 0.642 eV. In these graphs, an angle of 0° represents an exit trajectory perpendicular to the direction of the dimer rows, or parallel to the Si−Si bond axis within a dimer, while 90° represents an exit trajectory parallel to the dimer rows. As was the case for measuring the angle relative to the surface normal, due to the normal incidence of our F_2 molecules, the symmetry of the surface causes some directions to be equivalent. Although the azimuthal angle can take on values between 0° and 360°, we will use the symmetry of the surface and express our data as being from 0° to 180°.

Figure 14 indicates that F atoms ejected during abstraction have some preference for angles near 0° or 180°, or perpendicular to the dimer rows. This is presumably due to the stiff nature of the out-of-plane bend in the Si−F−F complex, which aligns the incipient scattered F atom along the dangling bond

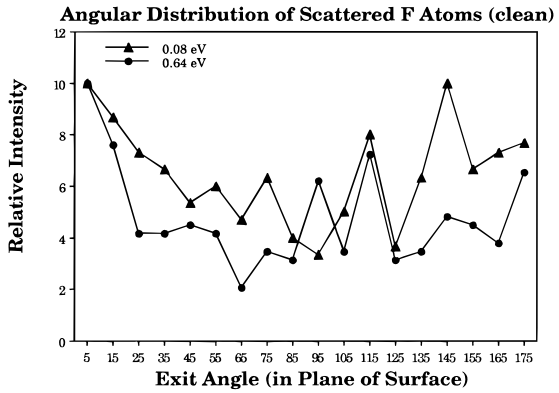

Figure 14. Azimuthal angular distribution of F atoms ejected during abstraction events for F_2 molecules impinging on the clean surface with 0.078 eV of incident translational kinetic energy. 0° and 180° are aligned with the direction of dangling bonds on the surface or perpendicular to the dimer rows, while 90° is parallel to the dimer rows on the surface.

direction. The preference for azimuthal angles perpendicular to the dimer rows is strongest for the low-incident energy case and is diminished for the higher-incident energy case. We suggest this is again a function of the sensitivity of the F_2 molecules to the potential energy surface, which diminishes as the incident energy increases. We note that experiments to detect such anisotropies in the azimuthal angular distributions should expect peaks at 0°, 90°, 180°, and 270°. On Si(100)-2×1 surfaces with low miscut angle, single atomic height steps will be present on the surface, leading to alternating p(2×1) and p(1×2) domains on the surface that have dimer rows which are perpendicular to each other. As a result, experimental measurements of the azimuthal exit angle will see the sum of the values for the p(2×1) and p(1×2) domains, for a total of four peaks.

IV. Implications for Etching

In the previous section, we provided an analysis of the dynamical details of the reaction mechanism as a function of fluorine coverage. In this section, we will suggest how to exploit the dynamical nature of the mechanism by using translationally activated molecular fluorine beams for new etching techniques, as well as implications that this mechanism has for understanding current limitations in anisotropic etching technology.

The goal in most plasma etching processes is to selectively etch the silicon surface. For this purpose, a relatively unreactive "mask" is placed over the regions of the surface where etching is not desired. In order to make smaller and smaller features on a silicon chip, the etching environment is optimized to yield anisotropic etching, where the etch rate perpendicular to the surface is much greater than the lateral etch rate. One of the constraints in improving current plasma etching processes is the problem of controlling undercutting of the etch mask due to lateral etching of the sidewalls of an etch feature.[9] When the lateral etch rate becomes too large relative to the perpendicular etch rate, a significant amount of etching can occur in the sidewalls of an etch feature, leading to loss of control over the size and shape of the feature.

Our simulations predict that F_2 has the critical characteristics necessary for successful use of translationally activated molecular beams of F_2 in neutral beam etching or related processes. First, we have seen that increasing the incident translational energy of the impinging F_2 molecules leads to increased reactivity over our entire range of incident energies and for all

surfaces we examined. Our simulations also indicate that F_2 molecules which scatter away from the surface without reaction have exit energies which are much smaller than their incident energies. This combination creates the possibility of using a focused, translationally activated beam of F_2 molecules to selectively react with a Si(100) surface, as any F_2 molecules which did not react with the surface on the first impact would have greatly reduced energy and thus might be unable to react elsewhere after scattering.

However, we must consider that the potential usefulness of F_2 molecular beams for reactions on the Si(100) surface might be mitigated by the stepwise nature of the reaction mechanism. As detailed above, our proposed mechanism predicts that when one of the F atoms in an F_2 molecule reacts to form an Si−F bond, if the other F atom is not subsequently chemisorbed nearby, it is ejected with little memory of its initial state. In particular, the energy of these ejected F atoms is relatively insensitive to the F_2 incident energy. Only the angle of ejection is significantly altered. Thus, translational activation of a beam of F_2 molecules primarily influences the formation of the first Si−F bond. Although increased translational energy in the impinging F_2 molecule depresses the angle of ejection of the second F atom toward the surface, it does not increase the ejection energy. As a result, when an F atom is ejected after a highly energetic F_2 molecule forms an Si−F bond, this F atom is more likely to stay near the surface and find an adjacent dangling bond site than an F atom ejected from a low-energy F_2 molecule, but it is not more likely to overcome a barrier to reaction if the site is already occupied. Thus, even at F_2 incident energies greater than 1 eV, our simulations suggest that atom abstraction could be an important or even dominant reaction pathway.

This abundance of scattered products poses potential problems for applications of F_2 molecular beams on Si(100) surfaces. For example, consider the reaction of F_2 molecules with the bottom of a trenchlike etch feature on the Si(100) surface. Any ejected F atoms or scattered F_2 molecules could react with the sidewalls of the feature, potentially leading to unwanted etching of these sidewalls and undercutting of the etch mask. A possible solution to this problem is to passivate the sidewalls of the feature. Earlier we mentioned our prediction that a barrier to reaction of 2−2.25 eV existed for F_2 molecules impinging on a Si(100) surface with an ordered monolayer of fluorine coverage. We have also found a barrier of 1−1.1 eV for atomic fluorine reacting with the same ordered surface.[46] If a similar ordered monolayer could be formed on the sidewalls, it might prevent reaction by species scattered away from the bottom of the etch feature. We are currently investigating this possibility.[46]

Even if a barrier to reactivity can be created for the sidewalls, our simulations indicate that the range of energies for ejected F atoms is fairly broad. For F_2 molecules impinging on our $\Theta_F = 1$ ML disordered surface with 4.0 eV of incident translational energy, we predicted that ejected F atoms may have energies as high as ∼3.0 eV at the edge of the distribution. However, experiments on the Si(100) surface indicate that the important quantity for reactivity is the translational energy directed normal to the surface. Previously, we noted that few F atoms were ejected from the surface at angles greater than 45° from the surface normal, leading to an angle of incidence with the sidewall of greater than 45° for the majority of the ejected F atoms. Even those F atoms ejected farthest from the surface normal will still only strike the sidewall at an incident angle of ∼30° from the sidewall normal. Based on normal energy scaling, this will lead to an effective incident energy of only $\cos^2(30)E_{tot}$, or $^3/_4E_{tot}$. Using the barrier to reactivity for F atoms on the $\Theta_F = 1$ ML ordered surface as a rough guide, only those ejected F atoms with greater than 1 eV of normal incident energy will be able to react with the sidewall, or $^4/_3(1.0\text{ eV}) = 1.33$ eV for the energy of F atoms impinging at the minimum angle of 30°. For 4.0 eV translationally excited F_2 molecules on the 1 ML disordered surface, less than 10% of the scattered F atoms had incident energies greater than 1.33 eV. Furthermore, preliminary simulations indicate that the barriers to reactivity for a passivated Si(110) surface may be significantly higher than those for the Si(100) surface (the likely exposed surface for the sidewalls of an etch feature).[46] Thus, most of the F atoms striking a passivated sidewall will be unable to react with it, as desired.

The same arguments presented here for neutral beam etching may also have bearing on the presence of sidewall undercutting in current plasma etching processes. Although F_2 is not thought to be a dominant specie in a fluorine-containing plasma, it may be present in small amounts. Given the high predicted rate of abstraction, any F_2 molecules present in the plasma that react with the bottom of the etch feature will generate a comparable number of ejected F atoms which all have >0.4 eV of energy. As detailed above, these F atoms will be targeted toward the sidewall, as few of the F atoms generated during abstraction leave along the direction of the surface normal. While this may not be a major cause of undercutting, it could be a contributing factor, suggesting that schemes which passivate the sidewalls of etch features against F atom attack may assist in the reduction of sidewall etching.

As for scattered F_2 molecules, our simulations predict that even for 4.0 eV incident F_2 molecules, the average exit energy of a scattered F_2 molecule is roughly the same as that of the F atoms ejected for the same initial conditions. As noted above, the barrier to reaction for F_2 on the $\Theta_F = 1.0$ ML ordered surface is ∼2.25 eV, more than twice the ∼1.0 eV barrier for F atoms reacting with the same surface. We have also already shown that any vibrational excitation of the scattered F_2 molecules should have a minimal effect on their reactivity. Based on the barriers to reactivity for the Si(100) surface, any passivation scheme which prevents reactivity with ejected F atoms should also work for scattered F_2. *Thus, we conclude from our dynamics that moderately translationally excited F_2 molecules may be effective at producing selective etching because the subsequent energy and hence reactivity of scattered F atom and F_2 byproducts should be greatly diminished.*

V. Summary

We have investigated the influence of up to 4.0 eV of translational excitation on the reactivity of F_2 molecules with the Si(100) surface. Although thermal F_2 molecules do not spontaneously etch the surface, our simulations indicate that translational kinetic energy is an effective control variable for greatly increasing the reactivity of F_2 molecules impinging on Si(100) surfaces. In our proposed reaction mechanism, increased COM translational kinetic energy enhances reactivity in two ways. When the presence of preadsorbed fluorine creates areas of the surface with a barrier to reactivity, higher translational kinetic energies allow a higher percentage of F_2 molecules either to find a nearby available dangling bond site or to penetrate the surface Si−F groups to form Si−F bonds with lower layer Si atoms. Once the first Si−F bond is formed, increased translational energy in the incident F_2 causes depression of the exit angle for F atoms ejected from the short-lived Si−F−F complex, allowing the ejected F atom to explore a greater region of the surface for favorable bonding sites before escaping. Those F atoms which do escape have hyperthermal

exit energies which appear to be only characteristic of repulsions in the Si−F−F exit channel, having little memory of the initial F_2 incident energy or the surface temperature. The ejection angle of these F atoms correlates with the direction of the axis of the newly formed Si−F bond on the surface. Scattered F_2 molecules, on the other hand, exhibit a moderate dependence on the F_2 incident kinetic energy, showing large but incomplete accommodation of this incident energy by the surface. The broad angular distribution of the scattered F_2 molecules is indicative of the corrugated nature of the Si(100) surface when $\Theta_F > 0$. While these scattered product trends are largely insensitive to the coverage of fluorine atoms on the surface, the partitioning between reaction channels is not. Even a coverage of $\Theta_F = 0.5$ ML leads to dramatic reduction in reactivity, and coverages of $\Theta_F = 1$ ML can prevent reaction altogether for ordered surfaces when the F_2 incident kinetic energy is <2.5 eV. The presence of disorder in the surface layer mitigates this effect, causing additional dangling bond sites to be available at a given coverage. These reaction characteristics potentially point to use of translationally activated F_2 beams in neutral beam etching applications, but further study is required to investigate the effects of scattered products in these applications.

It is also worth noting that a great deal of our predicted data can be experimentally verified. While some work has already been done to characterize the partitioning between reaction channels, especially on the clean surface, the trends we predict for the translational kinetic energies of scattered F atoms and F_2 molecules should be accessible via time-of-flight mass spectrometry measurements. This type of experiment could also verify the angular distribution data, although this is a more difficult challenge.

Acknowledgment. We are grateful to the Air Force Office of Scientific Research for primary support of this work. E.A.C. also acknowledges support from Olin Chemical Corporation, the Camille and Henry Dreyfus Foundation, and the Alfred P. Sloan Foundation for Young Investigator, Teacher−Scholar, and Research Fellow Awards, respectively. L.E.C. is grateful to the UCLA Department of Chemistry and Biochemistry for a Dissertation Year Fellowship.

References and Notes

(1) For a review of molecular beam studies on semiconductor surfaces, see: Yu, M.; DeLouise, L. A. *Surf. Sci. Rep.* **1994**, *19*, 289.

(2) For example: (a) Giapis, K. P.; Moore, T. A.; Minton, T. K. *J. Vac. Sci. Technol. A* **1995**, *13*, 959. (b) Levis, R. J.; Waltman, C. J.; Cousins, L. M.; Copeland, R. G.; Leone, S. R. *J. Vac. Sci. Technol. A* **1990**, *8*, 311. (c) Ninomiya, K.; Suzuki, K.; Nishimatsu, S.; Okada, O. *J. Appl. Phys.* **1985**, *58*, 1177.

(3) Joosten, G. P.; Vugts, M. J. M.; Spruijt, H. J.; Senhorst, H. A. J.; Beijerinck, H. C. W. *J. Vac. Sci. Technol. A* **1994**, *12*, 636.

(4) Lo, C. W.; Varekamp, P. R.; Shuh, D. K.; Durbin, T. D.; Chakarian, V.; Yarmoff, J. A. *Surf. Sci.* **1993**, *292*, 171.

(5) Lo, C. W.; Shuh, D. K.; Chakarian, V.; Durbin, T. D.; Varekamp, P. R.; Yarmoff, J. A. *Phys. Rev. B* **1993**, *47*, 15648.

(6) Lo, C. W.; Shuh, D. K.; Yarmoff, J. A. *J. Vac. Sci. Technol. A* **1993**, *11*, 2054.

(7) Haring, R. A.; Liehr, M. *J. Vac. Sci. Technol. A* **1992**, *10*, 802.

(8) McFeely, F. R.; Morar, J. F.; Shinn, N. D.; Landgren, G.; Himpsel, F. J. *Phys. Rev. B* **1984**, *30*, 764.

(9) Winters, H. F.; Coburn, J. W. *Surf. Sci. Rep.* **1992**, *14*, 161.

(10) Engstrom, J. R.; Nelson, M. M.; Engel, T. *Surf. Sci.* **1989**, *215*, 437.

(11) Li, Y. L.; Yang, J. J.; Ceyer, S. T., to be published, as referenced in ref 1 by Yu and Delouise.

(12) Li, Y. L.; Pullman, D. P.; Yang, J. J.; Tsekouras, A. A.; Gosalvez, D. G.; Laughlin, K. B.; Zhang, Z.; Schulberg, M. T.; Gladstone, D. J.; Mcgonigal, M.; Ceyer, S. T. *Phys. Rev. Lett.* **1995**, *74*, 2603.

(13) Ceyer and co-workers, to be published.

(14) Behringer, E. R.; Flaum, H. C.; Kummel, A. C. *J. Phys. Chem.* **1995**, *99*, 5533.

(15) Behringer, E. R.; Flaum, H. C.; Sullivan, D. J. D.; Masson, D. P.; Lanzendorf, E. J.; Kummel, A. C. *J. Phys. Chem.* **1995**, *99*, 12863.

(16) For example: (a) Szabo, A.; Engel, T. *J. Vac. Sci. Technol. A* **1994**, *12*, 648. (b) Teraoka, Y.; Nishiyama, I. *Appl. Phys. Lett.* **1993**, *63*, 3355. (c) Sullivan, D. J. D.; Flaum, H. C.; Kummel, A. C. *J. Phys. Chem.* **1993**, *97*, 12051. (d) Geuzebroek, F. H.; Babasaki, Y.; Tanaka, M.; Nakamura, T.; Namiki, A. *Surf. Sci.* **1993**, *297*, 141. (e) Campos, F. X.; Weaver, G. C.; Waltman, C. J.; Leone, S. R. *J. Vac. Sci. Technol. B* **1992**, *10*, 2217.

(17) Stillinger, F. H.; Weber, T. A. *Phys. Rev. B* **1985**, *31*, 5262.

(18) Stillinger, F. H.; Weber, T. A. *J. Chem. Phys.* **1988**, *88*, 5123.

(19) Weber, T. A.; Stillinger, F. H. *J. Chem. Phys.* **1990**, *92*, 6239.

(20) Wu, C. J.; Carter, E. A. *J. Am. Chem. Soc.* **1991**, *113*, 9061.

(21) Wu, C. J.; Carter, E. A. *Phys. Rev. B* **1992**, *45*, 9065.

(22) Weakliem, P. C.; Wu, C. J.; Carter, E. A. *Phys. Rev. Lett.* **1992**, *69*, 200, 1475.

(23) Weakliem, P. C.; Carter, E. A. *J. Chem. Phys.* **1993**, *98*, 737.

(24) Carter, L. E.; Khodabandeh, S.; Weakliem, P. C.; Carter, E. A. *J. Chem. Phys.* **1994**, *100*, 2277.

(25) Schoolcraft, T. A.; Diehl, M. A.; Steel, A. B.; Garrison, B. J. *J. Vac. Sci. Technol. A* **1995**, *13*, 1861.

(26) Carter, L. E.; Carter, E. A. *J. Vac. Sci. Technol. A* **1994**, *12*, 2235.

(27) Carter, L. E.; Carter, E. A. *Surf. Sci.* **1995**, *323*, 39.

(28) Schoolcraft, T. A.; Garrison, B. J. *J. Am. Chem. Soc.* **1991**, *113*, 8221.

(29) Barone, M. E.; Graves, D. B. *J. Appl. Phys.* **1995**, *77*, 1303.

(30) Feil, H.; Dieleman, J.; Garrison, B. *J. Appl. Phys.* **1993**, *74*, 1303.

(31) Radny, M. W.; Smith, P. V. *Surf. Sci.* **1994**, *301*, 97.

(32) Craig, B. I.; Smith, P. V. *Surf. Sci.* **1993**, *290*, L662.

(33) Craig, B. I.; Smith, P. V. *Surf. Sci.* **1992**, *262*, 235.

(34) Bennett, S. L.; Greenwood, C. L.; Williams, E. M. *Surf. Sci.* **1993**, *290*, 267.

(35) Johnson, A. L.; Walczak, M. M.; Madey, T. E. *Langmuir* **1987**, *4*, 277.

(36) Bozack, M. J.; Dresser, M. J.; Choyke, W. J.; Taylor, P. A.; Yates, J. T. *Surf. Sci.* **1987**, *184*, L332.

(37) Stich, I.; De Vita, A.; Payne, M. C.; Gillan, M. J.; Clarke, L. J. *Phys. Rev. B* **1994**, *49*, 8076.

(38) (a) Stich, I.; Payne, M. C.; De Vita, A.; Gillan, M. J.; Clarke, L. J. *Chem. Phys. Lett.* **1993**, *6*, 617. (b) De Vita, A.; Stich, I.; Gillan, M. J.; Payne, M. C.; Clarke, L. J. *Phys. Rev. Lett.* **1993**, *71*, 1276.

(39) Nosé, S. *Mol. Phys.* **1984**, *52*, 255.

(40) Hoover, W. G. *Phys. Rev. A* **1985**, *31*, 1695.

(41) Verlet, L. *Phys. Rev.* **1967**, *159*, 98.

(42) Hammersly, J. M.; Handscomb, D. C. *Monte Carlo Methods*; Wiley: New York, 1964.

(43) Jensen, J. A.; Yan, C.; Kummel, A. C. *Science* **1995**, *267*, 493.

(44) Huber, K. P.; Herzberg, G. *Molecular Spectra and Molecular Structure. IV. Constants of Diatomic Molecules*; Van Nostrand Reinhold: New York, 1979.

(45) Jensen, J. A.; Yan, C.; Kummel, A. C. *Phys. Rev. Lett.*, submitted.

(46) Carter, L. E.; Carter, E. A., to be published.

JP952905I